Hindawi Publishing Corporation
Discrete Dynamics in Nature and Society
Volume 2016, Article ID 4859475, 9 pages
http://dx.doi.org/10.1155/2016/4859475

Research Article

Application of H_∞ Filter on the Angular Rate Matching in the Transfer Alignment

Lijun Song, Zhongxing Duan, and Jiwu Sun

Electronic Information and Control Engineering College, Xi'an University of Architecture and Technology, Xi'an 710055, China

Correspondence should be addressed to Lijun Song; songlijun9071@sina.com

Received 7 December 2015; Accepted 17 February 2016

Academic Editor: Filippo Cacace

Copyright © 2016 Lijun Song et al. This is an open access article distributed under the Creative Commons Attribution License, which permits unrestricted use, distribution, and reproduction in any medium, provided the original work is properly cited.

The transfer alignment (TA) scheme is used for the initial alignment of Inertial Navigation System (INS) on dynamical base. The Kalman filter is often used in TA to improve the precision of TA. And the statistical characteristics of interference signal which is difficult to get must be known before the Kalman filter is used in the TA, because the interference signal is a random signal and there are some changes on the dynamic model of system. In this paper, the H_∞ filter is adopted in the TA scheme of the angular rate matching when the various stages of disturbance in measurement are unknown. And it is compared with the Kalman filter in the same environment of simulation and evaluation. The result of simulation shows that the H_∞ filter and the Kalman filter are both effective. The Kalman filter is more accurate than the H_∞ filter when system noise and measurement noise are white noise, but the H_∞ filter is more accurate and quicker than the Kalman filter when system noise and measurement noise are color noise. In the engineering practice, system noise and measurement noise are always color noise, so the H_∞ filter is more suitable for engineering practice than the Kalman filter.

1. Introduction

TA of airborne missile strapdown inertial system is the initial alignment that the attitude, velocity, and position of the Master Inertial Navigation System (MINS) are used by the Slave Inertial Navigation System (SINS). TA estimated the real data of misalignment angle of SINS by the Kalman filter. In theory, in the high precision strapdown inertial navigation system, the angular rate of the air-body with inertial spatial coordinate frame is measured by the gyro of MINS or the gyro of SINS, and the data of gyro of MINS should be the same as the data of gyro of SINS when the random drift of gyro of SINS is removed. But the error of gyro is always existence between MINS and SINS because there are installation error and wing flexibility [1].

According to the fundamental principle of the alignment, the method of transfer alignment may be divided into two kinds; one is called calculated parameter matching, such as velocity matching, attitude matching, and position matching; the other is called measuring parameter matching, such as acceleration matching and angular rate matching. Each has advantages and disadvantages, respectively [2, 3].

(1) The calculated parameter matching has high precision, because the influence of the vibration environment of the vehicle can be effectively inhibited. But the measuring parameter matching does not have high precision, because the precision of measuring parameter matching is greatly affected by airborne wing flexibility and flutter, and it is difficult to get the accurate model of airborne wing flexibility and flutter.

(2) The calculated parameter matching needs the long time to alignment, because it needs the long time to get the data of measurement difference; but the measuring parameter matching is more fast, because the measuring parameter matching uses the data from inertial components which can be got directly from the inertial components.

Before the middle of the 1980s, the researcher was mainly focused on the theory of Kamle filter's model and the method of TA. The basic methods of TA were velocity matching and position matching, and there were many literatures for these. In addition, Schneider proposed and combined the angular rate matching and the acceleration matching

which were formed by the measuring parameter matching.

In the late 1980s and 1990s, to receive the rapid transfer alignment method, the researcher was mainly focused on the rapid transfer alignment method and interference factor of precision of TA. Kain and Cloutier [4] proposed velocity and attitude matching of TA which is based on the model of velocity matching at first in 1989. This method could be used to achieve rapid transfer alignment, and it was one of the most popular methods for rapid transfer alignment. The velocity and attitude matching only used a simple wave instead of S maneuver which is always used in the velocity matching. The simple trajectory could reduce the difficulty of maneuver and shorten the alignment time. Soon after, Rogers proposed velocity and angular rate matching of TA in 1991 and compared it with velocity and attitude matching of TA. The result of research showed that the velocity and angular rate matching and the velocity and attitude matching could effectively shorten the alignment time, but the sensitivity of noise to the velocity and angular rate matching was more sensitive than the velocity and attitude matching. And after the middle of the 1990s, TA had been applied in the weapon and has been used as an application [5, 6].

In this paper, the work pays attention to study of filter of TA to improve the precision and effectiveness of the initial alignment of INS.

2. The Principle of the Angular Rate Matching

In general, the high precision strapdown inertial navigation system is used in MINS, and the lower precision strapdown inertial navigation system than MINS is used in SINS. The system of SINS is installed on the airborne missile, so it is also called the airborne missile strapdown inertial system. The airborne missile strapdown inertial system could use the angular rate matching because the strapdown inertial navigation system could get the angular rate directly. The main advantage of the angular rate matching is that the time of TA is short and fast, but it has some disadvantages; the first is that the alignment precisions is lower than velocity matching, because the alignment precisions of angular rate matching is influenced by installation error, the wing flexibility, flutter, and so on.

The wing flexibility usually is the flexibility of the wing, the launcher, and the external store. In theory, in order to attain the prediction of the elastic deformation, the aeroelastic model will use the aeroelasticity theory to be derived by the structural stiffness, the material properties, and the aerodynamics characteristic of the wing, the launcher, and the external store, and it is very complicated and effected by the position and the weight of the external store. The aeroelastic model is very significant for the study of Kalman filter, but the robustness of Kalman filter is very bad because there are many minimal damp modal and uncertainties of flight conditions. So the paper uses one good robustness filter for the rapid TA, which is the H_∞ filter; the H_∞ filter could successfully estimate the error of TA but it did not need to predict and estimate the flexibility of the wing [7, 8].

Figure 1 is the airborne missile suspended under the wing. M is the position of MINS, S is the position of SINS, and

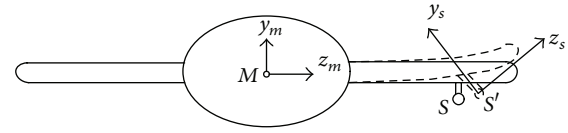

Figure 1: The airborne missile suspended under the wing.

MSNS ($O_m x_m y_m z_m$) and SINS ($O_s x_s y_s z_s$) are all strapdown inertial navigation system.

The angular rate matching used the error data of gyro between MINS and SINS as measurement. Misalignment angles of attitude are modified after the installation error of missile body and the flexure deformations of wing are estimated by the Kalman filter [9, 10]. Assume that $\widetilde{\boldsymbol{\omega}}_{ib_m}^{b_m}$ is the data of MINS's gyro, $\widetilde{\boldsymbol{\omega}}_{ib_s}^{b_s}$ is the data of SINS's gyro, $\boldsymbol{\mu}$ is installation error angle of missile body, and $\boldsymbol{\lambda}_f$ is flexure deformation angle of wing. The principle diagram of angular rate matching is as shown in Figure 2.

3. The Algorithm of H_∞ Suboptimal Filter

At present, the Kalman filter is used as traditional method of TA. In essence, the error of misalignment angle and inertial instruments are used as state variable of Kalman filter, and estimated by optimal estimation method to reduce the error of misalignment angle and inertial instrument. The precision and speed of TA are determined by the state variable. But the Kalman filter must have the linear of system model. If the system model is approximately linear, the Kalman filter would converge and estimate the state variable. But if the system model is not approximately linear, the Kalman filter would have great error, even leading to divergence. The H_∞ filter is a new technology for filtering, which is suitable for the nonlinear system and has higher estimating precision than the Kalman filter [11, 12]. The H_∞ suboptimal filter is an optimizing filter. In order to take the norm of H_∞ as optimizing performance, the norm of H_∞ is minimized between the disturbance input and filtering output.

The statistical characteristics of interference signal and dynamic model of system must be known before use in the Kalman filter. But it is difficult to know the statistical characteristics of interference signal because it is random signal in the actual system and there are some changes on the dynamic model of system. For the uncertainty of the statistical characteristics of interference signal and dynamic model of system, the H_∞ suboptimal filter constructs the norm of H_∞ [13, 14].

It is assumed that the system equation and measurement equation of linear discrete system can be written as

$$\begin{aligned} \mathbf{X}_k &= \boldsymbol{\phi}_{k,k-1}\mathbf{X}_{k-1} + \boldsymbol{\Gamma}_{k-1}\mathbf{W}_{k-1}, \\ \mathbf{Z}_k &= \mathbf{H}_k\mathbf{X}_k + \mathbf{V}_k, \end{aligned} \tag{1}$$

where $\mathbf{X}_k$ is estimated state, $\mathbf{Z}_k$ is the measurement of system, and $\boldsymbol{\phi}_{k,k-1}$ is transfer matrix from t_{k-1} to t_k. $\boldsymbol{\Gamma}_{k-1}$ is input matrix of system disturbance and $\mathbf{W}_{k-1}$ is noise sequence of

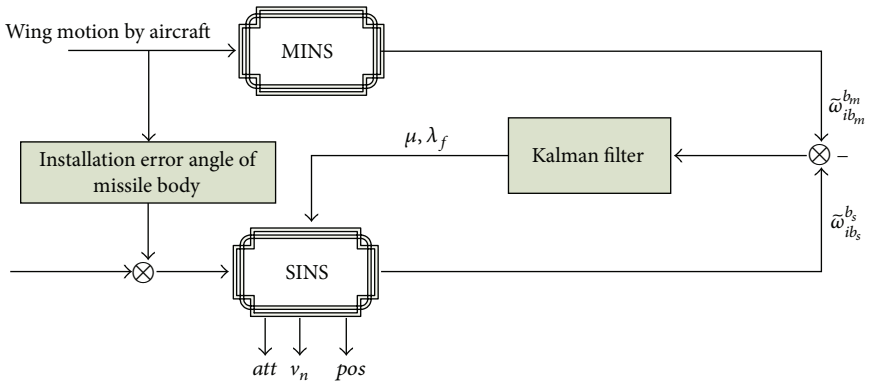

Figure 2: The principle diagram of angular rate matching.

system incentive. $\mathbf{H}_k$ is the measurement matrix and $\mathbf{V}_k$ is noise sequence of measurement.

Linearization of system state vector is estimated by measurement matrices, such as the following:

$$\mathbf{S}_k = \mathbf{L}_k \mathbf{X}_k, \tag{2}$$

where $\mathbf{L}_k$ is linear transform matrix of status vector.

It is supposed that $\widehat{\mathbf{S}}_{k/k} = \mathbf{F}(\mathbf{Z}_0, \mathbf{Z}_1, \mathbf{Z}_2, \ldots, \mathbf{Z}_k)$ is the estimate of $\mathbf{S}_k$ from t_0 to t_k. So $\widetilde{\mathbf{S}}_k$ is described as

$$\widetilde{\mathbf{S}}_k = \widehat{\mathbf{S}}_{k/k} - \mathbf{L}_k \mathbf{X}_k. \tag{3}$$

It is supposed that $T_k(F)$ is transfer function matrix which forms the initial state error of $(\mathbf{X}_0 - \widehat{\mathbf{X}}_0)$ and the unknown disturbances of $\{\mathbf{W}_i\}_{i=0}^k$ and $\{\mathbf{V}_i\}_{i=0}^k$ to $\widetilde{\mathbf{S}}_k$.

The H_∞ suboptimal filter is made as $\|\mathbf{T}_k(\mathbf{F})\|_\infty < \gamma$ of $\widehat{\mathbf{S}}_{k/k} = \mathbf{F}_f(\mathbf{Z}_0, \mathbf{Z}_1, \mathbf{Z}_2, \ldots, \mathbf{Z}_k)$ when $\gamma > 0$; that is,

$$\sup_{\mathbf{x}_0, \mathbf{W}, \mathbf{V} \in h_2} \frac{\sum_{i=0}^k \left|\widetilde{\mathbf{S}}_{i/i}\right|^2}{\left(\mathbf{X}_0 - \widehat{\mathbf{X}}_0\right)^{\mathrm{T}} \mathbf{P}_0^{-1} \left(\mathbf{X}_0 - \widehat{\mathbf{X}}_0\right) + \sum_{i=0}^k |\mathbf{W}_i|^2 + \sum_{i=0}^k |\mathbf{V}_i|^2} < \gamma^2, \tag{4}$$

where $\mathbf{X}_0$ is the initial state of system, $\widehat{\mathbf{X}}_0$ is the estimation of $\mathbf{X}_0$, and $\mathbf{P}_0$ is error matrix of initial estimation, which is $\mathbf{P}_0 = E\{[\mathbf{X}_0 - \widehat{\mathbf{X}}_0][\mathbf{X}_0 - \widehat{\mathbf{X}}_0]^{\mathrm{T}}\}$.

When the system model is based on formula (1), $\gamma > 0$ is a given constant, and $[\mathbf{\Phi}_k \ \ \mathbf{\Gamma}_k]$ is row full rank; the sufficient and necessary conditions of formula (4) are

$$\mathbf{P}_j^{-1} + \mathbf{H}_j^{\mathrm{T}} \mathbf{H}_j - \gamma^{-2} \mathbf{L}_j^{\mathrm{T}} \mathbf{L}_j > 0, \quad j = 0, 1, 2, \ldots, k. \tag{5}$$

And solution of H_∞ suboptimal filter is

$$\begin{aligned}
\mathbf{R}_{e,j} &= \begin{bmatrix} \mathbf{I} & \mathbf{0} \\ \mathbf{0} & -\gamma^2 \mathbf{I} \end{bmatrix} + \begin{bmatrix} \mathbf{H}_j \\ \mathbf{L}_j \end{bmatrix} \mathbf{P}_j \begin{bmatrix} \mathbf{H}_j^{\mathrm{T}} & \mathbf{L}_j^{\mathrm{T}} \end{bmatrix}, \\
\mathbf{P}_{j+1} &= \mathbf{\Phi}_j \mathbf{P}_j \mathbf{\Phi}_j^{\mathrm{T}} + \mathbf{Q}_k \\
&\quad - \mathbf{\Phi}_j \mathbf{P}_j \begin{bmatrix} \mathbf{H}_j^{\mathrm{T}} & \mathbf{L}_j^{\mathrm{T}} \end{bmatrix} \mathbf{R}_{e,j}^{-1} \begin{bmatrix} \mathbf{H}_j \\ \mathbf{L}_j \end{bmatrix} \mathbf{P}_j \mathbf{\Phi}_j^{\mathrm{T}}, \\
\mathbf{K}_{j+1} &= \mathbf{P}_{j+1} \mathbf{H}_{j+1}^{\mathrm{T}} \left(\mathbf{I} + \mathbf{H}_{j+1} \mathbf{P}_{j+1} \mathbf{H}_{j+1}^{\mathrm{T}}\right)^{-1}, \\
\widehat{\mathbf{X}}_{j+1/j+1} &= \mathbf{\Phi}_j \widehat{\mathbf{X}}_{j/j} + \mathbf{K}_{j+1} \left(\mathbf{Z}_{j+1} - \mathbf{H}_{j+1} \mathbf{\Phi}_j \widehat{\mathbf{X}}_{j/j}\right),
\end{aligned} \tag{6}$$

where $j = 0, 1, 2, \ldots, k$ and the initial value of X is arbitrary constants.

Before the H_∞ filter is used, it must satisfy $\mathbf{P}_k^{-1} + \mathbf{H}_k^{\mathrm{T}} \mathbf{H}_k - \gamma^{-2} \mathbf{L}_k^{\mathrm{T}} \mathbf{L}_k > 0$, and the coefficients of linear combination $\mathbf{L}_k$ and matrix $\mathbf{R}_{e,k}$ must exit. The Kalman filter is the special case of the H_∞ filter; when $\gamma \to 0$, the H_∞ filter would simplify to the Kalman filter.

Suppose $\gamma \to \infty$, when $\mathbf{L}_k = \mathbf{H}_k$; then,

$$\begin{aligned}
\mathbf{R}_{e,k}^{-1} &= \left(\begin{bmatrix} \mathbf{I} & \mathbf{0} \\ \mathbf{0} & -\gamma^2 \mathbf{I} \end{bmatrix} + \begin{bmatrix} \mathbf{H}_k \\ \mathbf{H}_k \end{bmatrix} \mathbf{P}_k \begin{bmatrix} \mathbf{H}_k^{\mathrm{T}} & \mathbf{H}_k^{\mathrm{T}} \end{bmatrix} \right)^{-1} \\
&= \begin{bmatrix} \mathbf{I} & \mathbf{0} \\ \mathbf{0} & \mathbf{0} \end{bmatrix} - \begin{bmatrix} \mathbf{H}_k \\ \mathbf{0} \end{bmatrix} \left(\mathbf{H}_k^{\mathrm{T}} \mathbf{H}_k + \mathbf{P}_k\right)^{-1} \begin{bmatrix} \mathbf{H}_k^{\mathrm{T}} & \mathbf{0} \end{bmatrix} \\
&= \mathbf{I} - \mathbf{H}_k \left(\mathbf{H}_k^{\mathrm{T}} \mathbf{H}_k + \mathbf{P}_k\right)^{-1} \mathbf{H}_k^{\mathrm{T}}.
\end{aligned} \tag{7}$$

Thus,

$$\begin{aligned}
\mathbf{P}_{k+1} &= \mathbf{\Phi}_k \mathbf{P}_k \mathbf{\Phi}_k^{\mathrm{T}} + \mathbf{\Gamma}_k \mathbf{\Gamma}_k^{\mathrm{T}} \\
&\quad - \mathbf{\Phi}_k \mathbf{P}_k \begin{bmatrix} \mathbf{H}_k^{\mathrm{T}} & \mathbf{H}_k^{\mathrm{T}} \end{bmatrix} \mathbf{R}_{e,k}^{-1} \begin{bmatrix} \mathbf{H}_k \\ \mathbf{H}_k \end{bmatrix} \mathbf{P}_k \mathbf{\Phi}_k^{\mathrm{T}} = \mathbf{\Phi}_k \mathbf{P}_k \mathbf{\Phi}_k^{\mathrm{T}} \\
&\quad + \mathbf{\Gamma}_k \mathbf{\Gamma}_k^{\mathrm{T}} \\
&\quad - \mathbf{\Phi}_k \mathbf{P}_k \begin{bmatrix} \mathbf{H}_k^{\mathrm{T}} & \mathbf{H}_k^{\mathrm{T}} \end{bmatrix} \left(\mathbf{I} - \mathbf{H}_k \left(\mathbf{H}_k^{\mathrm{T}} \mathbf{H}_k + \mathbf{P}_k\right)^{-1} \mathbf{H}_k^{\mathrm{T}}\right) \\
&\quad \cdot \begin{bmatrix} \mathbf{H}_k \\ \mathbf{H}_k \end{bmatrix} \mathbf{P}_k \mathbf{\Phi}_k^{\mathrm{T}}.
\end{aligned} \tag{8}$$

The H_∞ filter can be rewritten as

$$\begin{aligned}
\mathbf{P}_k &= \mathbf{\Phi}_{k,k-1} \mathbf{P}_{k-1} \mathbf{\Phi}_{k,k-1}^{\mathrm{T}} + \mathbf{\Gamma}_k \mathbf{\Gamma}_k^{\mathrm{T}}, \\
\mathbf{P}_{k+1} &= \left(\mathbf{I} - \mathbf{K}_k \mathbf{H}_k\right) \mathbf{P}_k,
\end{aligned}$$

$$\mathbf{K}_{k+1} = \mathbf{P}_{k+1}\mathbf{H}_{k+1}^{\mathrm{T}}\left(\mathbf{I} + \mathbf{H}_{k+1}\mathbf{P}_{k+1}\mathbf{H}_{k+1}^{\mathrm{T}}\right)^{-1},$$
$$\widehat{\mathbf{X}}_{k+1} = \boldsymbol{\Phi}_k\widehat{\mathbf{X}}_k + \mathbf{K}_{k+1}\left(\mathbf{Z}_{k+1} - \mathbf{H}_{k+1}\boldsymbol{\Phi}_k\widehat{\mathbf{X}}_k\right). \tag{9}$$

This is the Kalman filter. It is the special case of the H_∞ filter; with γ continuous increase, the H_∞ filter would close to the Kalman filter until $\gamma \to \infty$. When $\gamma \to \infty$, the H_∞ filter would simplify as the Kalman filter, while matrix $\mathbf{Q}$ and matrix $\mathbf{R}$ are unit matrices. In this process, minimum variance estimation of state which is the optimal estimation of state can be obtained, but robustness of filter would get worse. With γ continuous decrease, the H_∞ filter is less sensitive to the change of error of system model, error of initial state, and statistical property of noises, but robustness of filter would gradually increase, variance of estimated state would become big, and the precision of estimation would gradually reduce [15, 16].

The different points between the H_∞ filter and the Kalman filter are as follows:

(1) The linear combination of state $\mathbf{L}_k\mathbf{X}_k$ depended on the H_∞ filter, but the linear estimation of Kalman filter is given by linear combination of state estimation.

(2) The H_∞ filter must satisfy $\mathbf{P}_k^{-1} + \mathbf{H}_k^{\mathrm{T}}\mathbf{H}_k - \gamma^{-2}\mathbf{L}_k^{\mathrm{T}}\mathbf{L}_k > 0$, but $\mathbf{L}_k$ does not exist in the Kalman filter, and $\mathbf{P}_k$ is always positive definite, so the Kalman filter does not need any condition.

(3) The H_∞ filter uses covariance matrix, but the Kalman filter uses unit array.

(4) The Kalman filter is the special case of the H_∞ filter; when $\gamma \to \infty$, the H_∞ filter would simplify to the Kalman filter. It represents that the H_∞ norm of Kalman filter becomes very big, so the robustness of Kalman filter would be become worse.

4. The State-Space Model of the Angular Rate Matching

In theory, the gyros of MINS and SINS all measure the angular velocity of the inertial space on the different position. When MINS is the high precision strapdown navigation system, if the gyro drift of SINS is removed, the data gyro of MINS and SINS should be the same. But it is not the same in fact because there is attitude misalignment angle which is caused by the installation error, the wing flexibility, and flutter [17, 18].

4.1. The State Equation of the Angular Rate Matching. It is supposed that $\mathbf{X}_\omega = \left[\boldsymbol{\mu}^{b_f\mathrm{T}} \ \boldsymbol{\lambda}_f^{b_m\mathrm{T}} \ \boldsymbol{\omega}_f^{b_m\mathrm{T}} \ \boldsymbol{\varepsilon}_b^{b_s\mathrm{T}}\right]^{\mathrm{T}}$ is system state of the angular rate matching, where $\boldsymbol{\mu}^{b_f} = \left[\mu_x^{b_f} \ \mu_y^{b_f} \ \mu_z^{b_f}\right]^{\mathrm{T}}$ is the error of missile body's installation angle and $\boldsymbol{\lambda}_f = \left[\lambda_{fx} \ \lambda_{fy} \ \lambda_{fz}\right]^{\mathrm{T}}$ is the flexure deformation angle of wing. $\boldsymbol{\omega}_f = \left[\omega_{fx} \ \omega_{fy} \ \omega_{fz}\right]^{\mathrm{T}}$ is the flexure deformation angular rate of wing; $\boldsymbol{\varepsilon}^{b_s} = \left[\varepsilon_x^{b_s} \ \varepsilon_y^{b_s} \ \varepsilon_z^{b_s}\right]^{\mathrm{T}}$ is gyro drift of SINS. State equation of the angular rate matching is

$$\begin{aligned}\dot{\boldsymbol{\mu}}^{b_f} &= \mathbf{0},\\ \dot{\boldsymbol{\lambda}}_f &= \boldsymbol{\omega}_f,\\ \dot{\boldsymbol{\omega}}_f &= -\left[\boldsymbol{\beta}^2\right]\boldsymbol{\lambda}_f - [\boldsymbol{\beta}]\boldsymbol{\omega}_f + \boldsymbol{\eta},\\ \dot{\boldsymbol{\varepsilon}}^{b_s} &= \mathbf{0}.\end{aligned} \tag{10}$$

So the state-space model of the angular rate matching is

$$\dot{\mathbf{X}}_\omega = \begin{bmatrix}\mathbf{0}_{3\times3} & \mathbf{0}_{3\times3} & \mathbf{0}_{3\times3} & \mathbf{0}_{3\times3}\\ \mathbf{0}_{3\times3} & \mathbf{0}_{3\times3} & \mathbf{I}_{3\times3} & \mathbf{0}_{3\times3}\\ \mathbf{0}_{3\times3} & -\left[\boldsymbol{\beta}^2\right] & -[\boldsymbol{\beta}] & \mathbf{0}_{3\times3}\\ \mathbf{0}_{3\times3} & \mathbf{0}_{3\times3} & \mathbf{0}_{3\times3} & \mathbf{0}_{3\times3}\end{bmatrix}\mathbf{X}_\omega + \begin{bmatrix}\mathbf{0}_{3\times1}\\ \mathbf{0}_{3\times1}\\ \boldsymbol{\eta}\\ \mathbf{0}_{3\times1}\end{bmatrix}, \tag{11}$$

where $\boldsymbol{\varepsilon}_w^{b_s}$ is the Gaussian white noise of gyro, $\boldsymbol{\eta} = \left[\eta_x \ \eta_y \ \eta_z\right]^{\mathrm{T}}$ is the Gaussian white noise sequence of second order, where $\boldsymbol{\eta}_i \sim \mathbf{N}(0, Q_i)$, $Q_i = 4\beta_i^3\sigma_\eta^2$, and σ_η^2 is the variance of flexure deformation angle; $[\boldsymbol{\beta}] = \mathrm{diag}\,(\beta_x, \beta_y, \beta_z)$ and $[\boldsymbol{\beta}^2] = \mathrm{diag}(\beta_x^2, \beta_y^2, \beta_z^2)$.

4.2. The Measurement Equation of the Angular Rate Matching. It is supposed that $\widetilde{\omega}_{ib_m}^{b_m}$ is the measurement of MINS's gyro, $\widetilde{\omega}_{ib_s}^{b_s}$ is the measurement of SINS's gyro, and $\mathbf{C}_{b_f}^{b_h}$ is installation matrix of missile body.

The relative rotation of missile body which is based on horizontal position is θ_s; θ_s is angle which is around longitudinal angle of the missile which is installed under the wing, so the installation matrix is

$$\mathbf{C}_{b_f}^{b_h} = \left(\mathbf{C}_{b_h}^{b_f}\right)^{\mathrm{T}} = \begin{bmatrix}\cos\theta_s & 0 & \sin\theta_s\\ 0 & 1 & 0\\ -\sin\theta_s & 0 & \cos\theta_s\end{bmatrix}. \tag{12}$$

Because the performance of gyro of MINS is better than SINS, which usually is of 2~3 orders, it is the true value of aircraft angular velocity, the same as angular velocity of MINS. The measurement of gyro of MINS and SINS can be obtained as

$$\begin{aligned}\widetilde{\boldsymbol{\omega}}_{ib_m}^{b_m} &= \boldsymbol{\omega}_{ib_m}^{b_m},\\ \widetilde{\boldsymbol{\omega}}_{ib_s}^{b_s} &= \boldsymbol{\omega}_{ib_s}^{b_s} + \boldsymbol{\varepsilon}_b^{b_s} + \boldsymbol{\varepsilon}_w^{b_s},\end{aligned} \tag{13}$$

where $\boldsymbol{\omega}_{ib_s}^{b_s}$ is the measurement of gyro of SINS, $\boldsymbol{\omega}_{ib_m}^{b_m}$ is the true measurement of gyro of MINS, $\boldsymbol{\varepsilon}_b^{b_s}$ is the constant drift of gyro of SINS, and $\boldsymbol{\varepsilon}_w^{b_s}$ is the Gaussian white noise sequence of gyro of SINS.

So measurement equation of the angular rate matching is

$$\begin{aligned}\mathbf{Z}_\omega &= \mathbf{C}_{b_f}^{b_h}\widetilde{\boldsymbol{\omega}}_{ib_s}^{b_s} - \widetilde{\boldsymbol{\omega}}_{ib_m}^{b_m} = \mathbf{C}_{b_f}^{b_h}\left(\boldsymbol{\omega}_{ib_s}^{b_s} + \boldsymbol{\varepsilon}_b^{b_s} + \boldsymbol{\varepsilon}_w^{b_s}\right) - \boldsymbol{\omega}_{ib_m}^{b_m}\\ &= \mathbf{C}_{b_f}^{b_h}\boldsymbol{\omega}_{ib_s}^{b_s} - \boldsymbol{\omega}_{ib_m}^{b_m} + \mathbf{C}_{b_f}^{b_h}\boldsymbol{\varepsilon}_b^{b_s} + \mathbf{C}_{b_f}^{b_h}\boldsymbol{\varepsilon}_w^{b_s}.\end{aligned} \tag{14}$$

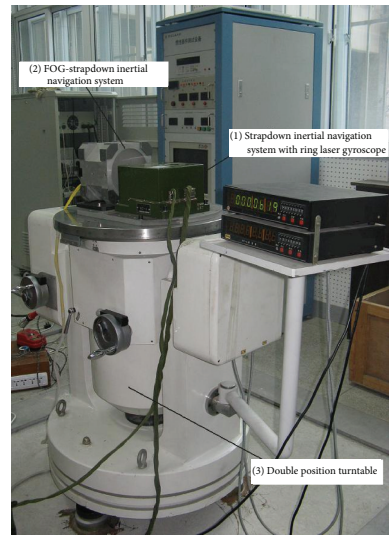

Figure 3: Experimental equipment installation diagram.

It is supposed that $\boldsymbol{\mu}^{b_f}$ is the installation error angle of missile body, $\boldsymbol{\lambda}^{b_m} = \boldsymbol{\lambda}_f^{b_m} + \boldsymbol{\lambda}_v^{b_m}$ is the elastic deformation angle of wing, where $\boldsymbol{\lambda}_f^{b_m}$ is the flexure deformation angle of wing and $\boldsymbol{\lambda}_v^{b_m}$ is the flutter deformation angle of wing, $\boldsymbol{\omega}_\lambda^{b_m} = \boldsymbol{\omega}_f^{b_m} + \boldsymbol{\omega}_v^{b_m}$ is the elastic deformation angular rate of wing, where $\boldsymbol{\omega}_f^{b_m}$ is the flexure deformation angular rate of wing and $\boldsymbol{\omega}_v^{b_m}$ is the flutter deformation angular rate of wing. So $\mathbf{C}_{b_f}^{b_h}\boldsymbol{\omega}_{ib_s}^{b_s}$ is such as

$$\begin{aligned}\mathbf{C}_{b_f}^{b_h}\boldsymbol{\omega}_{ib_s}^{b_s} &= \mathbf{C}_{b_f}^{b_h}\mathbf{C}_{b_f}^{b_s}\mathbf{C}_{b_h}^{b_f}\mathbf{C}_{b_m}^{b_h}\left(\boldsymbol{\omega}_{ib_m}^{b_m}+\boldsymbol{\omega}_f^{b_m}+\boldsymbol{\omega}_v^{b_m}\right)\\ &= \mathbf{C}_{b_f}^{b_h}\left[\mathbf{I}-\left(\boldsymbol{\mu}^{b_f}\times\right)\right]\mathbf{C}_{b_h}^{b_f}\left\{\mathbf{I}-\left[\left(\boldsymbol{\lambda}_f^{b_m}+\boldsymbol{\lambda}_v^{b_m}\right)\times\right]\right\}\\ &\cdot\left(\boldsymbol{\omega}_{ib_m}^{b_m}+\boldsymbol{\omega}_f^{b_m}+\boldsymbol{\omega}_v^{b_m}\right)\approx\boldsymbol{\omega}_{ib_m}^{b_m}+\boldsymbol{\omega}_f^{b_m}+\boldsymbol{\omega}_v^{b_m}\\ &-\mathbf{C}_{b_f}^{b_h}\left(\boldsymbol{\mu}^{b_f}\times\right)\mathbf{C}_{b_h}^{b_f}\boldsymbol{\omega}_{ib_m}^{b_m}-\boldsymbol{\lambda}_f^{b_m}\times\boldsymbol{\omega}_{ib_m}^{b_m}-\boldsymbol{\lambda}_v^{b_m}\times\boldsymbol{\omega}_{ib_m}^{b_m}.\end{aligned}\tag{15}$$

It can be obtained that

$$\begin{aligned}\mathbf{Z}_\omega &= -\mathbf{C}_{b_f}^{b_h}\left(\boldsymbol{\mu}^{b_f}\times\right)\mathbf{C}_{b_h}^{b_f}\boldsymbol{\omega}_{ib_m}^{b_m}+\boldsymbol{\omega}_{ib_m}^{b_m}\times\boldsymbol{\lambda}_f^{b_m}+\boldsymbol{\omega}_f^{b_m}\\ &+\mathbf{C}_{b_f}^{b_h}\boldsymbol{\varepsilon}_b^{b_s}+\mathbf{C}_{b_f}^{b_h}\boldsymbol{\varepsilon}_w^{b_s}+\boldsymbol{\omega}_v^{b_m}+\boldsymbol{\omega}_{ib_m}^{b_m}\times\boldsymbol{\lambda}_v^{b_m}\\ &=\boldsymbol{\omega}_{ib_m}^{b_m}\times\boldsymbol{\mu}^{b_f}+\boldsymbol{\omega}_{ib_m}^{b_m}\times\boldsymbol{\lambda}_f^{b_m}+\boldsymbol{\omega}_f^{b_m}+\mathbf{C}_{b_f}^{b_h}\boldsymbol{\varepsilon}_b^{b_s}+\mathbf{V}_\omega,\end{aligned}\tag{16}$$

where $\mathbf{V}_\omega$ is the Gaussian white noise sequence of the angular rate matching. It is such as

$$\mathbf{V}_\omega=\mathbf{C}_{b_f}^{b_h}\boldsymbol{\varepsilon}_w^{b_s}+\boldsymbol{\omega}_v^{b_m}+\boldsymbol{\omega}_{ib_m}^{b_m}\times\boldsymbol{\lambda}_v^{b_m}.\tag{17}$$

The measurement equation of system is

$$\mathbf{Z}_{\boldsymbol{\omega}}=\left[\boldsymbol{\omega}_{ib_m}^{b_m}\times\ \ \boldsymbol{\omega}_{ib_m}^{b_m}\times\ \ \mathbf{I}_{3\times3}\ \ \mathbf{C}_{b_f}^{b_h}\right]\mathbf{X}_{\boldsymbol{\omega}}+\mathbf{V}_{\boldsymbol{\omega}}.\tag{18}$$

5. The Semiphysical Simulation and Conclusion

Because the time of the airborne missile is relatively short, the precision of the airborne missile strapdown inertial system is almost determined by the precision of the TA but not the gyro drift which is too late to affect the precision of the navigation system. It is helpful to improve the scheme of TA and make an objective evaluation of the algorithm by the error of TA.

The semiphysical simulation of TA is that the data of the motion state and the inertial device is no longer from the simulation, but from the engineering practice of inertial navigation system which consists of the gyroscope and the accelerometer. The process of TA is to keep the necessary data of the gyroscope and accelerometer to be processed offline. The purpose of semiphysical simulation is to verify the effectiveness of the angular rate matching of TA.

5.1. The Experimental Equipment Installation. The experimental equipment installation diagram is shown in Figure 3. In the figure, the first is strapdown inertial navigation system with ring laser gyroscope, the second is FOG-strapdown inertial navigation system, and the last is the double position turntable. The strapdown inertial navigation system with ring laser gyroscope is high precision inertial navigation system; it is MINS of TA. The FOG-strapdown inertial navigation system is medium accuracy inertial navigation system; it is SINS of TA. The MINS and SINS are mounted on the double position turntable by chassis to realize the maneuver. The installation position of the strapdown inertial navigation system with ring laser gyroscope and the FOG-strapdown inertial navigation system are installed on the different position; the mutual-orientation relationship in 3 dimensions of them is that their x-axis, y-axis, and z-axis are parallel to each other, where x-axis is southward, y-axis is eastward, and z-axis is upward.

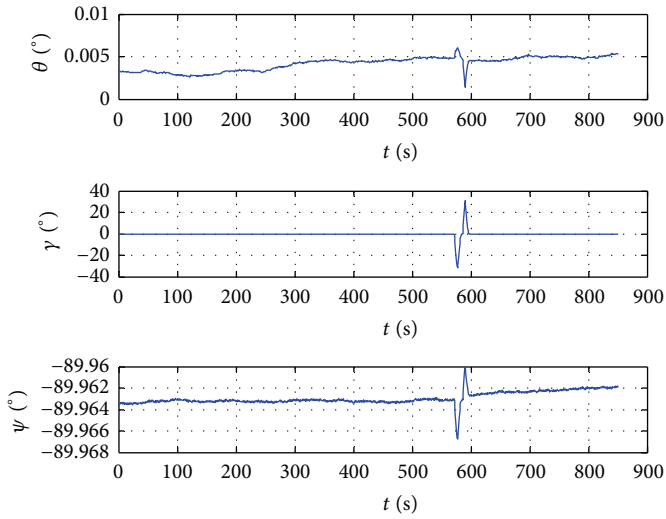

Figure 4: The change of attitude angle of semiphysical simulation.

5.2. The Maneuver Trajectory of Experiment. The controllability and observables of state variable are improved very slowly under the conditions of uniform level and accelerated level in TA. But they can effectively improve under the condition of turning maneuver and sinusoidal maneuver in TA. According to the fight characteristic, this paper makes the corresponding numerical simulation under wing motion by aircraft. The angle of shake wing is 30°. The initial position of TA is that north latitude is 34.03006°, east longitude is 108.76405°, and altitude is 448 m. The initial attitude of TA is that yaw is −90°, roll is 0°, and pitch is 0°. In order to achieve the angular rate matching in the static environment of the semiphysical simulation, the paper supposes the height of aircraft is 7000 m and the flight velocity is 230 m/s when the TA starts. The simulation trajectory of aircraft is designed as Table 1. The whole simulation time is 900 s, but the trajectory of the maneuver time is only 25 s. For the convenience of analysis, the paper used the data of 60 s which include the trajectory of the maneuver for offline analysis.

The change of attitude angle of semiphysical simulation is shown in Figure 4.

According to the analysis of matching method, the attitude matching and the angular rate matching are very sensitive to the wing flexibility. When the wing flexibility is not accuracy of system modeling, the error would cause performance degradation of the Kalman filter of angular rate matching. So when the Kalman filter of angular matching is used by TA, it must modify the attitude misalignment angle after the installation error and the wing flexibility are estimated in the angular rate matching.

In this paper, it is supposed that the wing flexibility is not accuracy of system modeling in the simulation, and the model of aircraft is not established when the H_∞ filter of the angular rate matching is simulated. Unknown measurement is not included in measurement noise of the angular rate matching, and the wing flexibility and flutter are not considered in TA. The condition of simulation is as follows.

The error parameters of SINS: the constant drift of gyro is $1^\circ/\mathrm{h}$, the random walk of gyro is $0.1^\circ/\sqrt{h}$, the constant offset error of accelerometer is 5×10^{-4} g, and the standard deviation of accelerometer is 5×10^{-5} g$\cdot\sqrt{s}$:

The initial value of misalignment angle is $\boldsymbol{\varphi}(0) = [0.1^\circ \ \ 0.1^\circ \ \ 0.5^\circ]^{\mathrm{T}}$.

The installation error of body is $\boldsymbol{\mu}^{b_f} = [0.1^\circ \ \ 0.1^\circ \ \ 0.1^\circ]^{\mathrm{T}}$.

The initial value of velocity error is $\delta\mathbf{V}_e^n(0) = [3\,\mathrm{m/s} \ \ 3\,\mathrm{m/s} \ \ 3\,\mathrm{m/s}]^{\mathrm{T}}$.

Meanwhile, it has the same conditions as the Kalman filter. The red solid line is the result of H_∞ filter, and the blue dashed line is the result of Kalman filter.

Analysis of simulation results is as follows:

(1) According to the theory of angular rate matching and the error equation of inertial navigation system, the installation error angle of missile body is embodied by rotation coupling of the angular velocity of carrier aircraft. Because the data of angular velocity is only in y-axis, it is effectively estimated only on the x-axis and z-axis which are the installation error angle of missile body. It is showed as in Figures 6(a) and 6(c).

(2) The angular rate matching cannot correctly estimate the misalignment angle of north, because it has been working with y-axis on the simulation of angular rate matching and the local geographic north coincided with y-axis. It is shown as Figure 5(b).

(3) The simulation results illustrate that the H_∞ filter and the Kalman filter are both effective. The H_∞ filter is more accurate and faster than the Kalman filter when system noise and measurement noise are the color noise. The H_∞ filter is an effectual estimation method

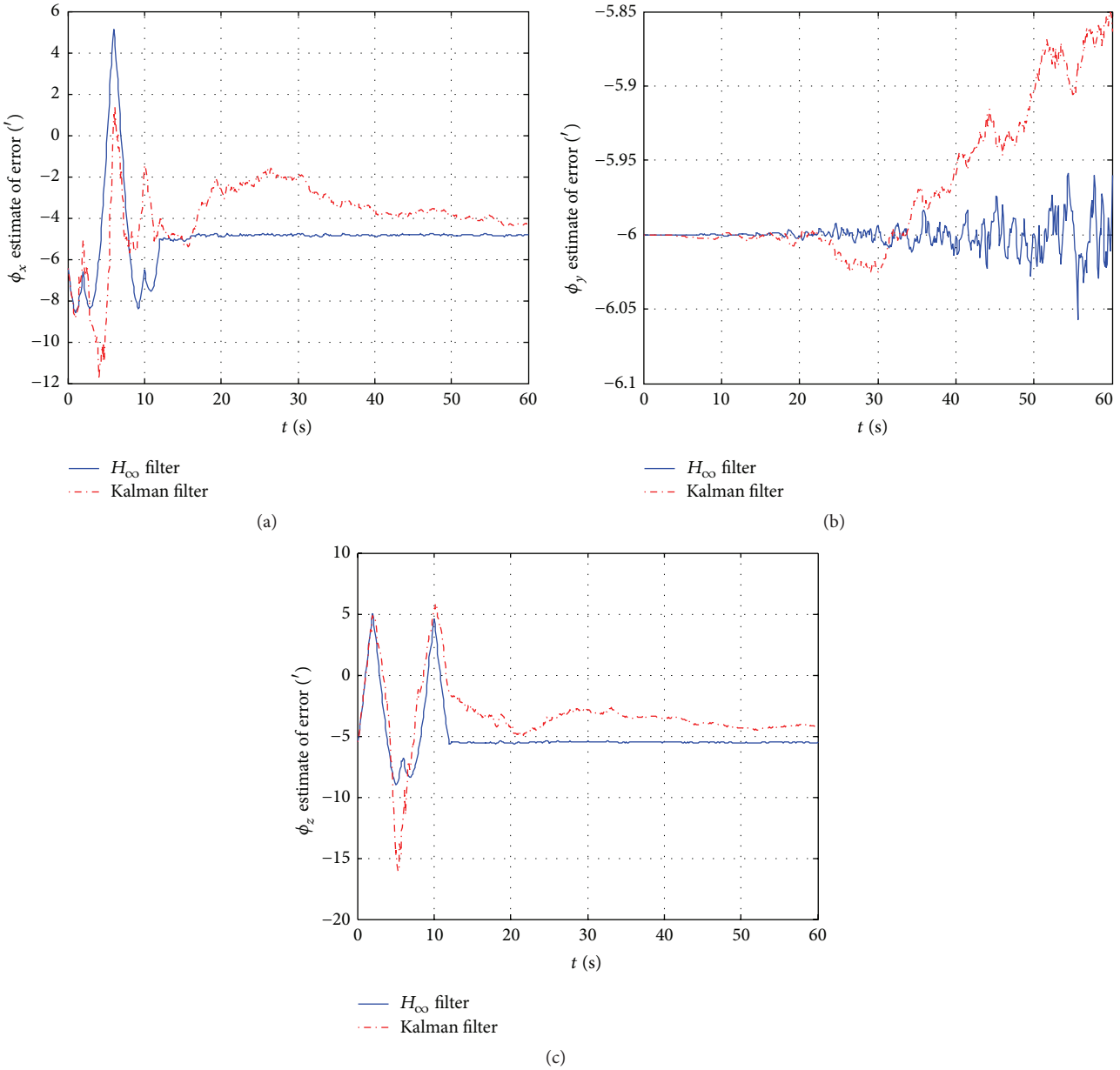

Figure 5: Estimate error of misalignment angle.

Table 1: Simulation trajectory of aircraft.

	Maneuver	Time of beginning (s)	Time of ending (s)	$\dot{\psi}$ (°/s)	$\dot{\theta}$ (°/s)	$\dot{\gamma}$ (°/s)
1	Uniform speed	0	572	0	0	0
2	Left deviation	572	577	0	0	−6°/s
3	Return	577	582	0	0	6°/s
4	Right deviation	587	592	0	0	6°/s
5	Return	592	597	0	0	−6°/s
6	Uniform speed	597	900	0	0	0

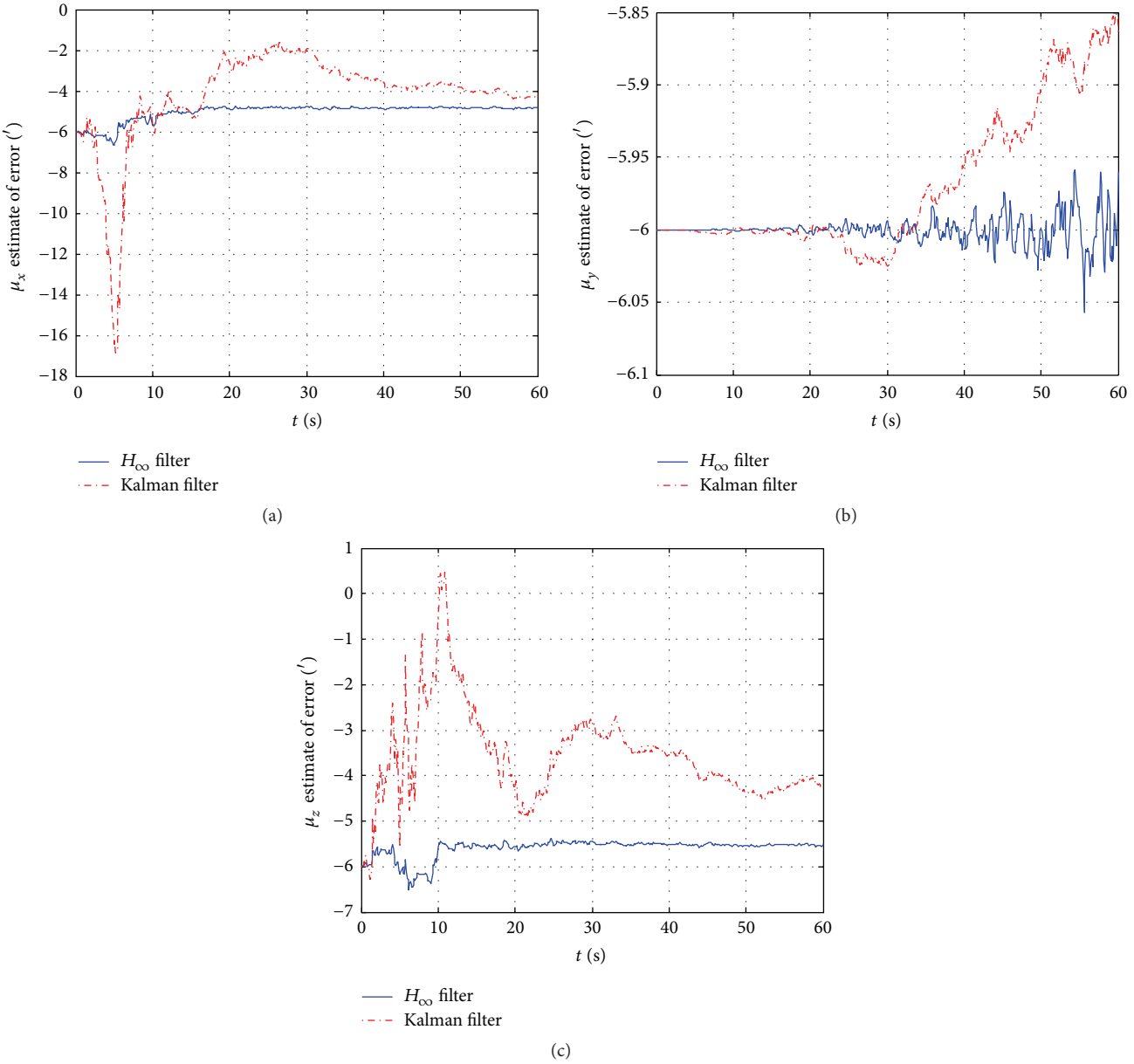

FIGURE 6: Estimate error of installation error angle.

compared to the Kalman filter because the noise of the engineering practice is mostly color noise. It is shown as in Figures 5(a) and 5(c). The convergence of misalignment angle of the H_∞ filter has been in $10'$ after 15 s, but the convergence of misalignment angle of the Kalman filter has been in $10'$ after 30 s.

(4) The missile body should be hanging in the wing root or fuselage, because it is very sensitive to flexure deformation on the angular rate match. This way can reduce the impact of flexure deformation and flutter deformation of wing when the angular rate matching is used to transfer alignment.

In the practical engineering applications, the system will be affected by the error of angular velocity and the wing flexure deformation, so the H_∞ filter is more suitable to engineering practice than Kalman filter.

Competing Interests

The authors declare that they do not have any commercial or associative interest that represents a conflict of interests in connection with the work submitted.

Acknowledgments

This work is partially supported by the special scientific research project of the Education Department of Shaanxi Provincial Government and the National Natural Science Foundation of China, Project nos. 15JK14 and 51178373.

References

[1] G.-L. Yang, L.-F. Wang, E.-K. Yuan, L. Cai, and L.-W. Qiao, "Rapid transfer alignment for carrier-based aircrafts in catapult," *Ship Science and Technology*, vol. 36, no. 3, pp. 50–54, 2014.

[2] C.-Y. Sun, *Transfer Alignment for Strapdown Inertial Navigation System*, Harbin Institute of Technology, Harbin, China, 2009.

[3] X.-J. Guan and X.-L. Wang, "Transfer alignment match methods for strapdown inertial navigation system on moving bases," *Aero Weapons*, vol. 4, no. 2, pp. 3–8, 2014.

[4] J. E. Kain and J. R. Cloutier, "Rapid transfer alignment for tactical weapon applications," in *Proceedings of the AIAA Guidance, Navigation and Control Conference*, pp. 1290–1300, Boston, Mass, USA, August 1989.

[5] Y. Wang and L.-W. Wang, "A transfer alignment method of SINS for shipborne torpedo," *Torpedo Technology*, vol. 18, no. 4, pp. 282–286, 2010.

[6] K. J. Shortelle, W. R. Graham, and C. Rabourn, "F-16 flight tests of a rapid transfer alignment procedure," in *Proceedings of the IEEE Position Location and Navigation Symposium*, pp. 379–386, Palm Springs, Calif, USA, April 1996.

[7] S. Majeed and J. Fang, "Performance improvement of angular rate matching shipboard transfer alignment," in *Proceedings of the 9th International Conference on Electronic Measurement and Instruments (ICEMI '09)*, vol. 3, pp. 706–711, Beijing, China, August 2009.

[8] H.-G. Liu, G. Chen, and C. Zhou, "Analysis of angular velocity matching transfer alignment for vessel," *Journal of Chinese Inertial Technology*, vol. 21, no. 5, pp. 565–569, 2013.

[9] H.-S. Ahn and C.-H. Won, "Fast alignment using rotation vector and adaptive Kalman filter," *IEEE Transactions on Aerospace and Electronic Systems*, vol. 42, no. 1, pp. 70–83, 2006.

[10] G.-M. Yan, J. Weng, P.-X. Yang, and Y.-Y. Qin, "Study on SINS rapid gyrocompass initial alignment," in *Proceedings of the International Symposium on Inertial Technology and Navigation*, Nanjing, China, October 2010.

[11] B. Feng, H. Ma, M. Fu, and C. Yang, "Real-time state estimator without noise covariance matrices knowledge-fast minimum norm filtering algorithm," *IET Control Theory & Applications*, vol. 9, no. 9, pp. 1422–1432, 2015.

[12] J.-H. Zhou and X.-H. Cheng, "The application of simplified UKF to initial alignment of SINS on swaying base," *Journal of Projectiles, Rockets, Missiles and Guidance*, vol. 26, no. 3, pp. 65–68, 2009.

[13] C. De Persis and A. Isidori, "An H_∞-suboptimal fault detection filter for bilinear systems," in *Nonlinear Control in the Year 2000*, A. Isidori, F. Lamnabhi-Lagarrigue, and W. Respondek, Eds., vol. 258 of *Lecture Notes in Control and Information Sciences*, pp. 331–339, Springer, New York, NY, USA, 2000.

[14] E. G. Collins Jr. and T. Song, "Robust H_∞ estimation and fault detection of uncertain dynamic systems," *Journal of Guidance, Control, and Dynamics*, vol. 23, no. 5, pp. 857–864, 2000.

[15] Y.-C. Lim and J. Lyou, "Transfer alignment error compensator design using H_∞ filter," in *Proceedings of the American Control Conference*, vol. 2, pp. 1460–1465, Anchorage, Alaska, USA, May 2012.

[16] A. Annamalai, A. Motwani, S. K. Sharma, R. Sutton, P. Culverhouse, and C. Yang, "A robust navigation technique for integration in the guidance and control of an uninhabited surface vehicle," *Journal of Navigation*, vol. 68, no. 4, pp. 750–768, 2015.

[17] E.-Z. Niu, J.-X. Ren, and J. Tan, "Design and analysis of simulation track in the test of strap-down inertial navigation system," *Computer Simulation*, vol. 26, no. 8, pp. 18–21, 2010.

[18] B. Luo, *The Research and Design of Transfer Alignment Simulation and Verification System on Ship Carried Weapon Inertial Navigation System*, Harbin Engineering University, Harbin, China, 2012.

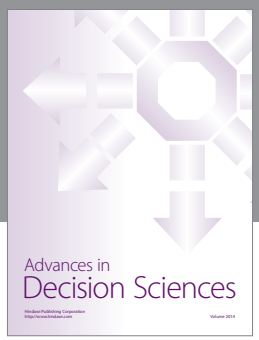

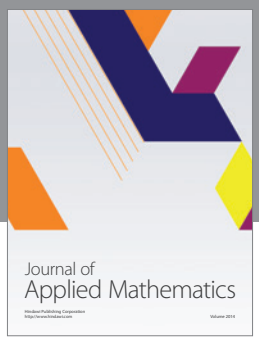

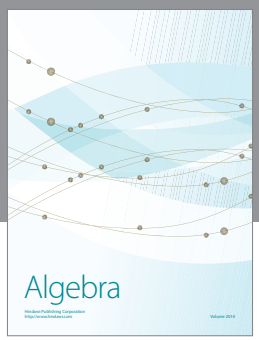

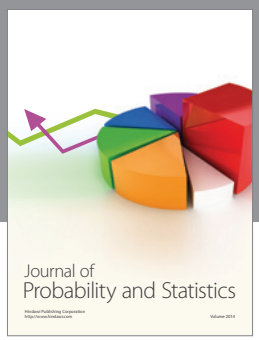

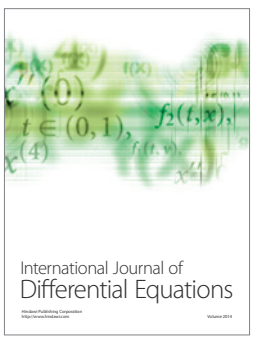

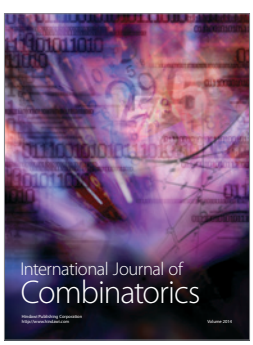

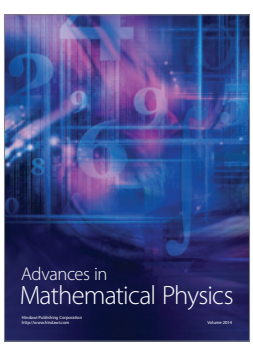

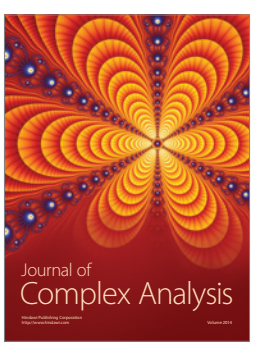

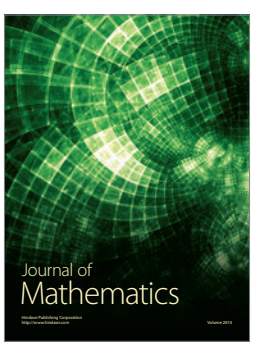

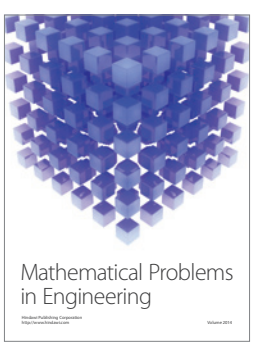

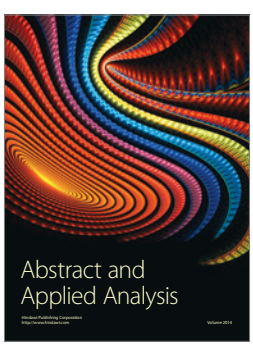

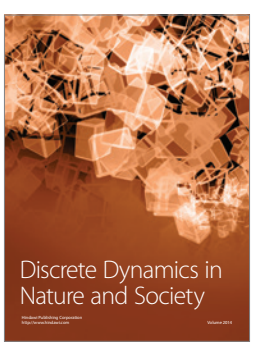

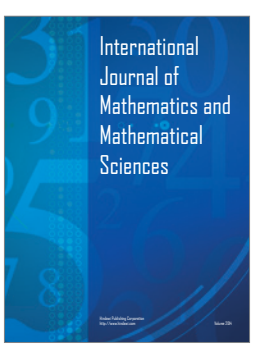

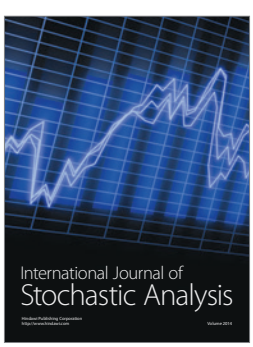

Hindawi

Submit your manuscripts at
http://www.hindawi.com